However, because of the proximity of markers used in this analysis, it is unlikely that more than one such event occurred over the region of interest among the entire set of backcross animals (male and female). Such undetected recombination events could not affect the order of loci that we determined or significantly alter the genetic distances we determined.
11. D. Vetrie *et al.*, *Nature* **361**, 226 (1993).
12. S. Tsukada *et al.*, *Cell* **72**, 279 (1993).
13. P. Sideras *et al.*, in preparation.
14. E. S. Kawasaki, in *PCR Protocols*, M. A. Innis, D. H. Gelfand, J. J. Sninsky, T. J. White, Eds. (Academic Press, San Diego, 1990), pp. 21–27. Cycle sequencing was done with the "Cyclist" kit (Stratagene). The sequences of primers used for this analysis are available from the authors.
15. J. M. Rossi *et al.*, *Proc. Natl. Acad. Sci. U.S.A.* **89**, 2456 (1992).
16. K. Kusumi, J. Smith, J. Segre, D. Koos, E. Lander, *Mamm. Genome*, in press.
17. M. C. Green and B. A. Witham, Eds., *Handbook on Genetically Standardized Jax Mice* (Jackson Laboratory, Bar Harbor, ME, 1991), pp. 14–15; *NIH Rodents* (National Institutes of Health, Bethesda, MD, 1980), pp. 18–21.
18. J. E. Coligan, A. M. Kruisbeek, D. H. Margulies, E. M. Shevach, W. Strober, Eds., *Current Protocols in Immunology*, (Wiley, New York, 1992), vol. 1, chaps. 3 and 8.
19. Immunoprecipitated material was washed twice with phosphate-buffered saline containing 0.5% NP-40 and 1 mM phenylmethylsulfonyl fluoride (wash buffer) and resuspended in 20 μl of kinase buffer [50 mM Hepes, 0.1 mM EDTA, 0.01% Brij35, bovine serum albumin (0.1 mg/ml), 10 mM dithiothreitol, 150 mM NaCl, 0.1 mM orthovanadate, and 10 mM NaF] to which 10 μl of 0.3 mM ATP and 48 mM $MgCl_2$ were added to initiate the reaction. After 20 min at room temperature, samples were washed twice with wash buffer and eluted in SDS-containing sample buffer.
20. D. L. Diuguid, M. J. Rabiet, B. C. Furie, B. Furie, *Blood* **74**, 193 (1989).
21. L. Prior *et al.*, *Am. J. Hum. Genet.* **51**, 143 (1992).
22. F. Lorenzo *et al.*, *Br. J. Haemotol.* **83**, 152 (1993).
23. M. E. Conley, *Annu. Rev. Immunol.* **10**, 215 (1992).
24. J. Sprent and J. Bruce, *J. Exp. Med.* **160**, 335 (1984).
25. H. H. Wortis, L. Burkly, D. Hughes, S. Roschelle, G. Waneck, *ibid.* **155**, 903 (1982); J. J. Mond *et al.*, *ibid.*, p. 924.
26. C. Bona, J. J. Mond, W. E. Paul, *ibid.* **151**, 224 (1980).
27. S. Desiderio, *Nature* **361**, 202 (1993).
28. M. P. Cooke and R. M. Perlmutter, *New Biol.* **1**, 66 (1988); M. M. Sugrue, J. S. Brugge, D. R. Marshak, P. Greengard, E. L. Gustafson, *J. Neurosci.* **10**, 2513 (1990); T. Dorai, J. B. Levy, L. Kang, J. S. Brugge, L. H. Wang, *Mol. Cell. Biol.* **11**, 4165 (1991).
29. Y. Ben-Neriah, A. Bernards, M. Paskind, G. O. Daley, D. Baltimore, *Cell* **44**, 577 (1986); W. S. Vincent, R. J. Gregory, S. C. Wadsworth, *Genes Dev.* **3**, 334 (1989); T. L. Yi, J. B. Bolen, J. N. Ihle, *Mol. Cell. Biol.* **11**, 2391 (1991).
30. F. R. Cross, E. A. Garber, D. Pellman, H. Hanafusa, *Mol. Cell. Biol.* **4**, 1824 (1984); M. P. Kamps, J. E. Buss, B. M. Sefton, *Proc. Natl. Acad. Sci. U.S.A.* **82**, 4625 (1985).
31. J.-Y. Kato *et al.*, *Mol. Cell. Biol.* **6**, 4155 (1986); J. S. Moyers, A. H. Bouton, S. J. Parsons, *ibid.* **13**, 2391 (1993).
32. R. A. Van Etten, P. Jackson, D. Baltimore, *Cell* **58**, 669 (1989).
33. Mano *et al.*, *Oncogene* **8**, 417 (1993); J. D. Siliciano, T. A. Morrow, S. V. Desiderio, *Proc. Natl. Acad. Sci. U.S.A.* **89**, 11194 (1992).
34. We thank J. Hu-Li, W. MacKenzie, C. Watson, B. Keitz, D. Swiatek, A. Morrow, D. Matthews, and M. Bruner for technical support; S. Rastan, S. Brown, and P. Avner for mouse X chromosome probes; S. Tsukada and O. Witte for antiserum to Btk; S. Tilghman and D. Koos for help with screening the Princeton Mouse YAC library; J. Inman for TNP-Ficoll; and G. Herman and A. Keegan for helpful discussions. Supported in part by a fellowship from the Helen Hay Whitney Foundation (to J.D.T.); grants from the Swedish Cancer Society and the Research Foundation of the Department of Oncology, University of Umeå (to P.S.); grants from the Swedish Medical Research Council, the Swedish Cancer Society, and the Axel and Margaret Ax:son Johnson Foundation (to C.I.E.S.); and NIH grants GM33160 and HG00277 (to V.C.).

19 April 1993; accepted 11 June 1993

Mutation of Unique Region of Bruton's Tyrosine Kinase in Immunodeficient XID Mice

David J. Rawlings, Douglas C. Saffran, Satoshi Tsukada, David A. Largaespada, J. Christopher Grimaldi, Lucie Cohen, Randolph N. Mohr, J. Fernando Bazan, Maureen Howard, Neal G. Copeland, Nancy A. Jenkins, Owen N. Witte*

The cytoplasmic tyrosine kinase, Bruton's tyrosine kinase (Btk, formerly bpk or atk), is crucial for B cell development. Loss of kinase activity results in the human immunodeficiency, X-linked agammaglobulinemia, characterized by a failure to produce B cells. In the murine X-linked immunodeficiency (XID), B cells are present but respond abnormally to activating signals. The Btk gene, *btk*, was mapped to the *xid* region of the mouse X chromosome by interspecific backcross analysis. A single conserved residue within the amino terminal unique region of Btk was mutated in XID mice. This change in *xid* probably interferes with normal B cell signaling mediated by Btk protein interactions.

B cell development is characterized by an orderly expression of cell surface markers and responses to specific activation signals (*1*). Tyrosine kinases are important in the signaling pathways regulating these events (*2*). Btk, expressed in B and myeloid cells, and several homologous genes constitute a unique tyrosine kinase subfamily distinct from the Src subfamily (*3*, *4*). The Btk family members have a long, highly conserved NH_2-terminal unique region and lack a negative regulatory tyrosine. Despite its critical role in B cell development, the specific functions of Btk in B cell signaling are not yet known.

The *xid* gene defect results in failure of B cells to become phenotypically and functionally diverse (*5*, *6*). B cells from XID mice do not respond to thymus-independent type 2 antigens, have abnormal responses to a variety of activation signals (*5–7*), and have a surface phenotype suggestive of disordered maturation (*8*). These findings suggest that B cells with the *xid* mutation lack essential signals for B cell activation and maturation. Despite characterization of these cellular defects, the underlying genetic change remains unknown.

In contrast to the *xid* mutation, X-linked agammaglobulinemia (XLA) results in production of few B cells and severe humoral immunodeficiency. Despite this distinction, XLA and XID have several common features. First, the surface phenotypes of XLA and XID B cells are similar, suggesting that both result in abnormal B cell activation (*6*, *9*). Second, both disorders appear to result from an intrinsic B lineage defect, as evidenced by nonrandom X chromosome inactivation limited to B cells (*10*). And finally, *xid* maps to a region of the X chromosome that shares homology with the human XLA locus at Xq21.3-Xq22 (*11*, *12*). For these reasons, we evaluated the possible role of Btk in XID.

The murine chromosomal location of *btk* was determined by interspecific backcross analysis using a mapping panel typed for over 1100 loci (*13*). Southern (DNA) blot analysis using a *btk* unique region probe identified three *Mus spretus*–specific Sph I restriction fragment length polymorphisms. These were used to follow the segregation of the *btk* locus in backcross mice (Fig. 1). The *btk* locus was mapped to the distal portion of the X chromosome linked to *pgk-1*, *DXPas2*, and *plp*. The gene order and recombination frequencies expressed in centimorgans (cM ± SE) are centromere, *pgk-1* (1.7 ± 1.7), *DXPas2* (3.6 ± 2.1), *btk* (3.3 ± 1.9), and *plp* (Fig. 1). The *xid* locus is distal to *Pgk-1* in the interval surrounding *DXPas2* (in Fig. 1) (*12*). These two data

D. J. Rawlings, D. C. Saffran, R. N. Mohr, Department of Microbiology and Molecular Genetics, University of California, Los Angeles, CA 90024.
S. Tsukada, L. Cohen, O. N. Witte, Howard Hughes Medical Institute, University of California, Los Angeles, CA 90024.
D. A. Largaespada, N. G. Copeland, N. A. Jenkins, Mammalian Genetics Laboratory, ABL–Basic Research Program, National Cancer Institute–Frederick Cancer Research and Development Center, Frederick, MD 21702.
J. C. Grimaldi, J. F. Bazan, M. Howard, DNAX Research Institute of Molecular and Cellular Biology, Palo Alto, CA 94304.
*To whom correspondence should be addressed.

sets, including the one in which we have placed *btk* near *DXPas2*, overlap at the 95% confidence interval and support the hypothesis that Btk is the mutated protein at the *xid* locus.

We then determined whether Btk expression was altered in mice carrying the *xid* mutation. CBA/N (*xid*) and CBA/J (+/+) spleen mononuclear cell lysates were immunoprecipitated with antiserum to murine Btk (*3*). Equivalent amounts of full-sized [^{35}S]methionine Btk and Btk autokinase activity were detected in both strains (Fig. 2A). To eliminate the contribution of Btk expression from myeloid cells, we evaluated pre-B cell lines derived from CBA/N and CBA/J animals after transformation of bone marrow with the v-*mos* oncogene (*14*). Flow cytofluorometric analysis of these lines was consistent with outgrowth of pre-B cell populations (Fig. 2C). All lines produced equivalent Btk autokinase activity (Fig. 2B).

Because Btk expression and in vitro kinase activity were unaltered in B cells from XID mice, we searched for mutations that could alter its ability to confer a signal—but not affect protein production, stability, or kinase activity. Polymerase chain reaction (PCR) products encoding overlapping *btk* gene products were generated with first strand cDNA template from CBA/N (*xid*) bone marrow and a series of oligonucleotide primers spanning the coding sequence of the gene (Fig. 3). Products were subcloned, sequenced, and compared to the cDNA sequence obtained from (C57BL/6 × DBA/2) F_1 mice (GenBank L08967). Three single-nucleotide changes were detected: C to T at nucleotide position 219 (*15*), C to T at position 881, and T to C at position 1829. The latter two changes did not result in amino acid alterations.

The nucleotide change at position 219 was predicted to change Arg^{28} to Cys^{28} in the unique region of Btk. This nucleotide change was confirmed in four independent overlapping products with different sets of PCR primers. Four additional clones obtained by PCR of cDNA from a different cell population and murine strain, splenic BALB.*xid* B cells, also contained this single-nucleotide change.

Seven exons comprise the Btk NH_2-terminal region coding sequence. The nucleotide change at position 219 is located within the first coding exon. Coding exons 1 to 5 were present within a 20-kb genomic clone Btk-D (Fig. 3, bottom). Exon-specific PCR was done with oligonucleotide primers specific to the intron-exon boundaries of *btk* exon 1. The results confirmed the Arg to Cys change in CBA/N. Sequence analysis of five additional murine strains, CBA/CaH-T6J, CBA/CaJ, CBA/J, BALB/c, and 129/Sv all demonstrated the wild-type consensus sequence. The CBA/CaH-T6J substrain contains the closest X chromosome progenitor for the *xid* mutation (*16*). These results are consistent with the Arg to Cys change being unique to CBA/N (*xid*).

Because of its complex exonic structure, the possibility that altered *btk* mRNA splice variants might be important in XID was evaluated. A series of reverse transcriptase PCR reactions with primer sets designed to amplify products spanning multiple *btk* unique region exons were carried out. Prod-

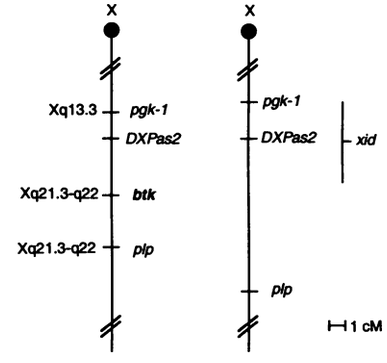

Fig. 1. The *btk* gene maps to the region of the *xid* mutation. The *btk* gene was placed in the distal region of the mouse X chromosome by interspecific backcross analysis (*22*). (**Left**) Partial X chromosome interspecific map showing the location of *btk* in relation to linked genes. The position of these loci on the human X chromosome are noted. (**Right**) The partial murine X chromosome map derived from a composite map from the mouse X chromosome committee (*12*). The approximate location of *xid* is shown. The maps are aligned at the *DXPas2* locus.

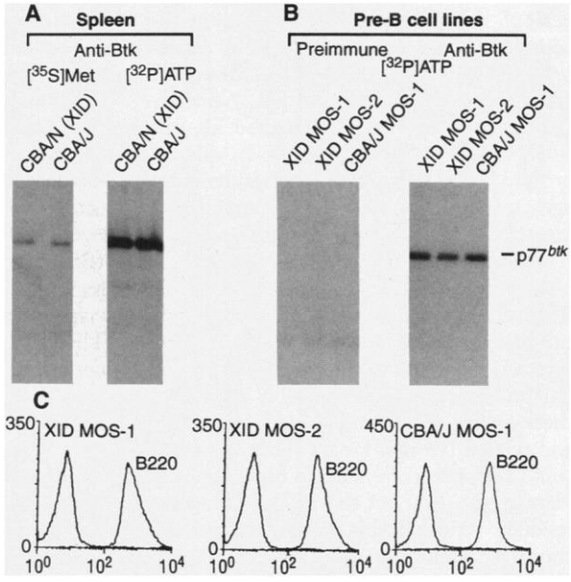

Fig. 2. Btk protein expression and in vitro kinase activity in CBA/J (+/+) and CBA/N (XID) tissues and pre-B cell lines. (**A**) Analysis of Btk protein expression in spleen mononuclear cells. (Left) Expression of Btk protein. CBA/J and CBA/N spleen mononuclear cells were labeled in vitro with 100 μCi of [^{35}S]methionine, and lysates were immunoprecipitated with antiserum to Btk (*3*). (Right) In vitro autokinase activity was assayed in the presence of [γ-^{32}P]adenosine triphosphate (*23*). (**B**) Btk in vitro kinase activity in pre-B cell lines. Location of the 77-kD Btk protein is indicated by a bar. (**C**) Expression of the B cell surface marker, B220, on CBA/J and (two independently derived) CBA/N pre-B cell lines. CBA/J and CBA/N bone marrow cells were infected with v-*mos* retrovirus (*14*) and plated as previously described (*24*). Cells were stained with phycoerythrin (PE)-coupled monoclonal antibody RA3-6B2 (anti-B220; Pharmingen) (right peak) or immunoglobulin G2a isotype control (left peak). Staining for Mac-1 was indistinguishable from control staining. Analyses were done on FACScan (Becton Dickinson).

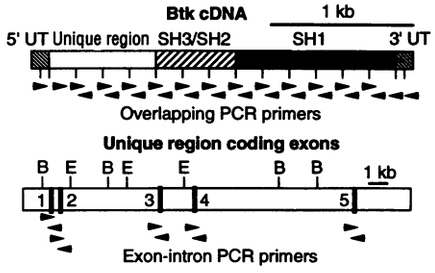

Fig. 3. PCR and sequence analysis of *btk* gene in CBA/N (*xid*). (**Top**) Location of PCR primers for amplification of overlapping *btk* cDNA products. Location of sense (forward arrows) and antisense (reverse arrows) primers (*25*) and *btk* unique region and SH domains are indicated. (**Bottom**) *btk* coding exons and *btk* exon-specific PCR primers. Partial restriction map (B, Bam HI; E, Eco RI) of Btk genomic clone indicating location of coding exons (1 to 5) and intron-exon–specific PCR primers. Bars represent 1 kb (*26*). Total RNA was isolated from CBA/N bone marrow with RNAzol (Biotext) and reverse-transcribed into cDNA with reverse transcriptase and random hexamers (*27*). The cDNA was amplified by PCR with *btk*-specific primer sets (*25, 28*), and the products were cloned into the TA vector (Invitrogen) and then sequenced with SP6 and T7 sequencing primers. Genomic DNA was amplified by PCR with *btk* exon 1–specific primers (5′-ATGGCTGCAGTGATACTG-3′ and 5′-TGGGAAACTTACCCCACGTTC-3′; intronic sequence underlined), cloned, and sequenced as above. [Note: A mistake in the reported murine cDNA sequence was identified, and a correction has been sent to GenBank (P123 is R)].

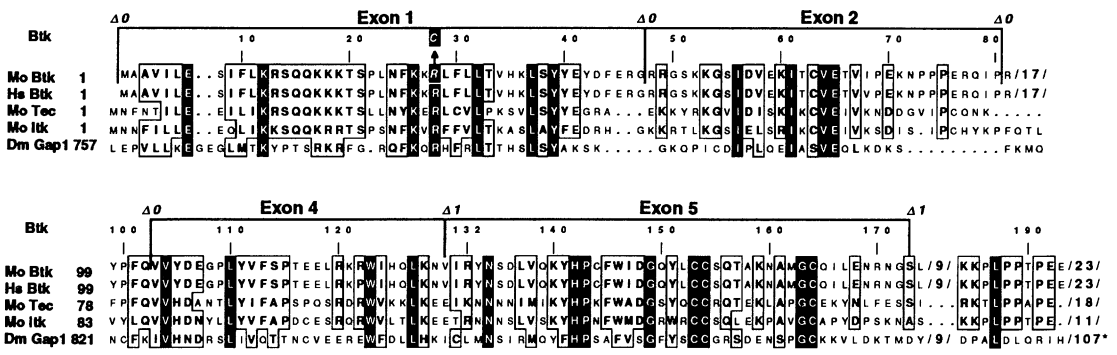

Fig. 4. Location of the Arg^{28} mutation and alignment of NH_2-terminal unique region residues of Btk subfamily members and *Drosophila* Gap1. Reverse contrast letters represent identical residues between human and murine Btk (Hs Btk; Mo Btk), murine tecII (Mo Tec), murine itk (Mo Itk), and *Drosophila* Gap1 (Dm Gap1). Boxes and bold letters indicate amino acids that are identical or conserved between four of the five sequences. The Arg^{28}-equivalent residues are italicized, and the upward arrow points to the Arg^{28}Cys mutation present in *xid*. The /**n**/ symbols indicate the number of residues in two insertions in Hs and Mo Btk and the chain distance between the unique domains and the adjoining SH3 domain; in Gap1, **107*** indicates the chain length to the COOH-terminus. The location of exons 1, 2, 4, and 5 of murine Btk are indicated; the Δ0 and Δ1 denote the type of intron boundary (between codons, or after the first codon position). Alignment was carried out using the PROFILE program (*29*). Single-letter abbreviations for the amino acids are as follows: A, Ala; C, Cys; D, Asp; E, Glu; F, Phe; G, Gly; H, His; I, Ile; K, Lys; L, Leu; M, Met; N, Asn; P, Pro; Q, Gln; R, Arg; S, Ser; T, Thr; V, Val; W, Trp; and Y, Tyr.

ucts of the predicted size, including the complete *btk* unique region, were consistently amplified from XID and normal pre-B and splenic B cells. In addition, Northern (RNA) blotting has not detected alternatively spliced mRNAs from pre-B, splenic, or Ly-1^+ B cells (*17*). These results argue against the presence of other mutational mechanisms affecting Btk in XID mice.

Identification of the Arg^{28} Btk mutation in XID mice and the failure of XID B cells to respond to activation signals suggest a central role for Btk in B cell signaling. Protein interactions involving the Btk NH_2-terminal unique region are probably critical to these events. The unique segments of Btk and related tyrosine kinase subfamily members (Tec and Itk) exhibit a high degree of identity (*3*). Sixty of the 179 superimposed residue positions in this chain are completely conserved, and the majority map to two discrete regions (amino acids 1 to 80, encoded by *btk* exons 1 and 2; and amino acids 103 to 172, encoded by exons 4 and 5) separated from each other and the Src homology (SH) domains by acidic proline-rich linkers (Fig. 4). The Arg^{28} residue is located in the first conserved block and is present in all the kinase subfamily members. This residue (and a neighboring conserved residue, Lys^{26}; Fig. 4) forms part of a locally hydrophilic stretch of amino acids. It is predicted that Arg^{28} lies on a loop segment following an α helix (residues 9 to 18 in Btk numbering) and leading into a hydrophobic β strand (residues 29 to 32) (*18*). Thus, the likely effect of the Arg^{28} to Cys mutation is the replacement of a surface-exposed, functionally important side chain.

The Btk unique region is related to a domain of unknown function in the *Drosophila* guanosine triphosphatase (GTPase) activating protein Gap1 [amino acids 755 to 950 (*19*)] that neighbors the GAP-homology module (Fig. 4). Gap1 is implicated in the control of signaling through the *Drosophila* Sevenless receptor tyrosine kinase by down-regulation of Ras1 activity (*19*). Perhaps the homology between the Btk unique region and the GAP-associated domain defines a previously uncharacterized "adaptor" module involved in analogous protein interactions within divergent signaling pathways.

The distinct genetic alterations in XLA (Btk kinase deficiency) and XID (unique region point mutation) provide clues toward the role of Btk in B cell development. The Arg^{28} mutation provides indirect evidence that these signals are mediated, in part, through interactions of the Btk unique region with other elements of the signal transduction pathway. In nude *xid* mice, progenitor B cell development is arrested (*20*), indicating that T cell–dependent factors are required to provide alternative signals to overcome the *xid* defect. In the absence of these factors, the Arg^{28} unique region mutation results in arrested B cell development. Study of these overlapping signals will be important in understanding overall control of B cell development.

Taken together, our data implicate the Arg^{28} Btk mutation in XID. Final proof, and test of the predicted role for the Btk unique region in B cell signaling, will require replacement of the defective gene.

REFERENCES AND NOTES

1. A. Rolink and F. Melchers, *Cell* **66**, 1081 (1991); R. R. Hardy, *Sem. Immunol.* **2**, 197 (1990); E. A. Clark and P. J. L. Lane, *Annu. Rev. Immunol.* **9**, 97 (1991).
2. A. L. DeFranco, *Eur. J. Biochem.* **210**, 381 (1992).
3. S. Tsukada *et al.*, *Cell* **72**, 279 (1993).
4. D. Vetrie *et al.*, *Nature* **361**, 226 (1993); R. J. Gregory, K. L. Kammermeyer, W. S. Vince, S. G. Wadsworth, *Mol. Cell. Biol.* **7**, 2119 (1987); H. Mano, F. Ishikawa, J. Nishida, H. Hirai, F. Takaku, *Oncogene* **5**, 1781 (1990); J. D. Siliciano, T. A. Morrow, S. V. Desiderio, *Proc. Natl. Acad. Sci. U.S.A.* **89**, 11194 (1992); S. D. Heyeck and L. J. Berg, *ibid.* **90**, 669 (1993); H. Mano *et al.*, *Oncogene* **8**, 417 (1993).
5. I. Scher, *Adv. Immunol.* **33**, 1 (1982).
6. L. S. Wicker and I. Scher, *Curr. Top. Microbiol. Immunol.* **124**, 87 (1986).
7. Y. Hitoshi *et al.*, *Int. Immunol.*, in press; N. F. Go *et al.*, *J. Exp. Med.* **172**, 1625 (1990).
8. R. R. Hardy, K. Hayakawa, D. R. Parks, L. A. Herzenberg, *Nature* **306**, 270 (1983); D. E. Mosier, *J. Mol. Cell. Immunol.* **2**, 70 (1985).
9. M. E. Conley, *J. Immunol.* **134**, 3070 (1985).
10. M. E. Conley *et al.*, *N. Engl. J. Med.* **315**, 564 (1986); M. H. Nahm, J. W. Paslay, J. M. Davie, *J. Exp. Med.* **158**, 920 (1983); L. M. Forrester, J. D. Ansell, H. S. Micklem, *ibid.* **165**, 949 (1987).
11. A. L. Hillyard, D. P. Doolittle, M. T. Davisson, T. H. Roderick, *Mouse Genome* **90**, 8 (1992).
12. S. D. M. Brown, P. Avner, G. E. Herman, *Mamm. Genome* **3**, S274 (1992).
13. N. G. Copeland and N. A. Jenkins, *Trends Genet.* **7**, 113 (1991).
14. R. Weiss *et al.*, *RNA Tumor Viruses. Molecular Biology of Tumor Viruses* (Cold Spring Harbor Laboratory, Cold Spring Harbor, NY, ed. 2, 1984).
15. Btk coding sequence starts at nucleotide 137 (GenBank L08967).
16. Staff of the Jackson Laboratory, *Handbook on Genetically Standardized JAX Mice* (Jackson Laboratory, Bay Harbor, ME, ed. 4, 1990), p. 9.
17. D. J. Rawlings, D. C. Saffran, S. Tsukada, O. N. Witte, unpublished data.
18. B. Rost and C. Sander, *Nature* **360**, 540 (1992); S. A. Benner, *Curr. Opin. Struc. Biol.* **2**, 402 (1992).
19. U. Gaul, G. Mardon, G. M. Rubin, *Cell* **68**, 1007 (1992).
20. H. Y. Chung, Z. Dong, H. H. Wortis, *J. Immunol.* **149**, 3456 (1992).
21. M. Gribskov, R. Luthy, D. Eisenberg, *Methods Enzymol.* **183**, 146 (1990); E. L. Green, in *Genetics and Probability in Animal Breeding Experiments* (Oxford Univ. Press, New York, 1981), p. 77.
22. Interspecific backcross progeny were generated by mating (C57BL/6J × *M. spretus*) F_1 females and C57BL/6J males as described (*13*). A total of 205 N2 mice were used to map the *btk* locus. Southern hybridization was done with a 0.6-kb *btk* unique region cDNA probe with a final wash at 65°C in 1× sodium chloride–sodium citrate, 0.1% SDS. The presence or absence of three cosegregating *M. spretus*–specific Sph I fragments (11.0, 7.6, and 2.0 kb) was followed in the backcross mice. We calculated recombination distances as described, using the computer program SPRETUS MADNESS (*21*). We determined gene order by minimizing the number of recombination events required to explain the allele distribution patterns.
23. T. Takemori *et al.*, *EMBO J.* **6**, 951 (1987); J. B. Konopka and O. N. Witte, *Mol. Cell. Biol.* **5**, 3116 (1985).
24. J. McLaughlin, E. Chianese, O. N. Witte, *Proc.*

Natl. Acad. Sci. U.S.A. **84**, 6558 (1987); C. A. Whitlock and O. N. Witte, *ibid.* **79**, 3608 (1982).
25. A series of 24 18-nucleotide primers with complete identity to the murine Btk cDNA sequence (GenBank L08967) were used to generate 380–base pair overlapping products spanning the entire *btk* coding sequence. Full sequence information is available from the authors.
26. Filter lifts containing 5×10^5 plaques from a 129/Sv murine genomic λ phage library were screened with a 0.6-kb unique region murine cDNA probe as described (*3*). Clones Btk-C and Btk-D were evaluated by restriction mapping, subcloned into pGEM7ZF(+), and partially sequenced by Sequenase (U.S. Biochemical) with T7, SP6, and *btk* unique region oligonucleotide primers.
27. E. S. Kawasaki, in *PCR Protocols: A Guide to Methods and Applications*, M. A. Innis *et al.*, Eds. (Academic Press, San Diego, 1990), pp. 21–27.
28. M. A. Innis and D. H. Gelfand, in *ibid.*, pp. 3–12; R. K. Saiki *et al.*, *Science* **230**, 1350 (1985).
29. We thank P. Soriano for the 129/Sv genomic library; J. Thomas, W. Paul, and collaborators for sharing prepublication data; C. Sawyers, S. Smale, and R. Wall for critical reading of the manuscript; and J. Shimaoka and K. Vensel for assistance in manuscript preparation. Supported by National Institutes of Health Immunology Training Grant, the Jonsson Comprehensive Cancer Center, and NIH Grant AR36834 (D.J.R.); Howard Hughes Medical Institute (D.C.S., S.T., L.C., and O.N.W.) and the Leukemia Society of America (D.C.S.); Schering-Plough (J.C.G., J.F.B., and M.H.); and the National Cancer Institute, Department of Health and Human Services, under contract N01-CO-74101 with Advanced BioScience Laboratory (D.A.L., N.G.C., and N.A.J.).

16 April 1993; accepted 10 June 1993

Cellular Mechanisms of a Synchronized Oscillation in the Thalamus

Marcus von Krosigk, Thierry Bal, David A. McCormick*

Spindle waves are a prototypical example of synchronized oscillations, a common feature of neuronal activity in thalamic and cortical systems in sleeping and waking animals. Spontaneous spindle waves recorded from slices of the ferret lateral geniculate nucleus were generated by rebound burst firing in relay cells. This rebound burst firing resulted from inhibitory postsynaptic potentials arriving from the perigeniculate nucleus, the cells of which were activated by burst firing in relay neurons. Reduction of γ-aminobutyric acid$_A$ (GABA$_A$) receptor–mediated inhibition markedly enhanced GABA$_B$ inhibitory postsynaptic potentials in relay cells and subsequently generated a slowed and rhythmic population activity resembling that which occurs during an absence seizure. Pharmacological block of GABA$_B$ receptors abolished this seizure-like activity but not normal spindle waves, suggesting that GABA$_B$ antagonists may be useful in the treatment of absence seizures.

Synchronized neuronal oscillations have been observed in thalamocortical networks during slow wave sleep (*1*, *2*), sensory processing (*3*), and generalized seizures (*4*). Spindle waves are one example of these neuronal oscillations and occur during the early stages of slow wave sleep. They appear as 7- to 12-Hz oscillations that wax and wane in amplitude over a 2- to 4-s period and that reappear once every 3 to 10 s (*1*, *2*). These synchronized oscillations are generated in the thalamus and depend on activity in the GABA-containing neurons of the thalamic reticular nucleus (nRt) or perigeniculate nucleus (PGN), although their dependence on the activity of relay neurons is unclear (*2*). The cellular bases of spindle wave generation are not only important for understanding thalamic function and the generation of the electroencephalogram during sleep but are also relevant to the understanding of generalized epilepsy, because the cellular mechanisms that generate absence seizures appear to be similar to those that generate spindle oscillations (*4*). We have studied the cellular mechanisms of spindle wave generation in thalamic slices and the transformation of these oscillations by GABA$_A$ receptor antagonists into activity resembling that of absence seizures.

Section of Neurobiology, Yale University School of Medicine, New Haven, CT 06510.

*To whom correspondence should be addressed.

Intracellular and extracellular multiple unit recordings from sagittal, coronal, or horizontal slices (*5*) from the dorsal lateral geniculate nucleus (LGNd) of ferrets revealed the spontaneous occurrence of spindle waves (Fig. 1, A and E). These in vitro spindle waves were recorded in the PGN and all three laminae of the LGNd (A, A1, and C). They recurred with a regularity of one every 3 to 30 s (typically 10 to 20 s) and were characterized by a within spindle frequency of 5 to 9 Hz (typically 6 to 7 Hz; Figs. 1B and 2A) (*6*).

Intracellular recordings from LGNd relay cells during spindle waves revealed a rhythmic occurrence of inhibitory postsynaptic potentials (IPSPs) (*7*), a few of which were followed by rebound bursts of action potentials (Fig. 1C; $n = 88$ cells). These

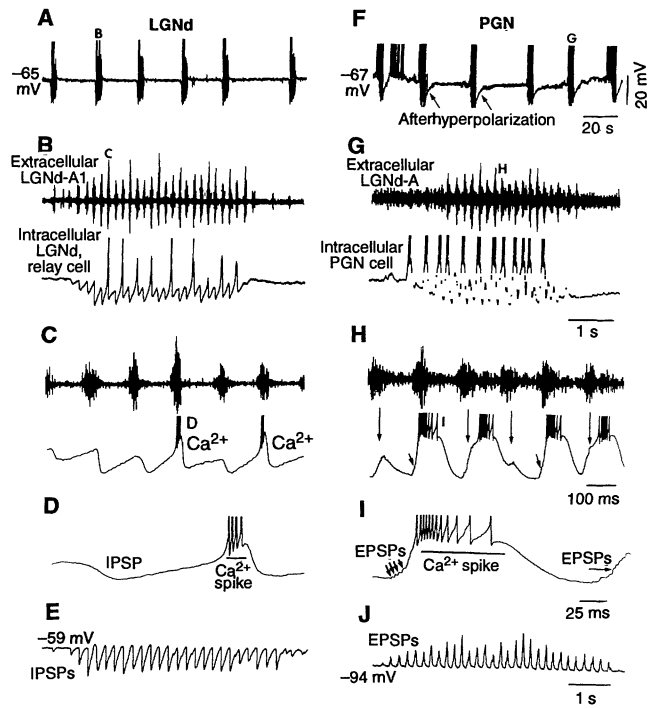

Fig. 1. Spindle oscillations in ferret geniculate slices. Letter labels in individual panels refer to a subsequent panel of higher temporal resolution. (**A**) Intracellular recording from an LGNd relay cell in lamina A revealed the recurrence of spindle waves approximately once every 20 s. (**B** to **D**) Detail of one spindle wave and parts of the spindle wave recorded both intracellularly in a relay neuron and locally as extracellular multiple unit activity in the LGNd. (**E**) Depolarization to −59 mV with intracellular injection of current completely inactivated the low threshold Ca^{2+} current and revealed the barrage of IPSPs associated with a spindle wave. (**F**) Intracellular recording from a morphologically identified PGN GABAergic cell during spindle wave generation. (**G**) Expansion of one spindle wave in the PGN cell and the simultaneously recorded multiple unit activity in lamina A. (**H**) Close examination of the simultaneous recordings from (G) revealed that each burst of activity in the relay lamina was associated with a barrage of EPSPs in the PGN cell. This barrage of EPSPs then activated, on occasion, a low threshold Ca^{2+} spike and a high-frequency burst discharge. (**I**) In some cases groups of three to five EPSPs arrived at the same frequency at which relay cells generated action potentials during a burst [compare (D) and (I)]. (**J**) Hyperpolarization of PGN cells to −94 mV prevented the activation of low threshold Ca^{2+} spikes and revealed the underlying barrages of EPSPs. Spindle oscillations were successfully recorded in at least one slice in 78 out of 85 experiments.